ANALYSIS OF THE PERFORMANCE OF A LOW-POWER ATMOSPHERIC BURNER FOR GAS APPLIANCES FOR HOUSEHOLDS AND THEIR IMPACT ON THE EMISSION AND STABILITY OF THE BURNER

by

Aleksandar M. MILIVOJEVIĆ[*], Miroljub M. ADŽIĆ, Milan D. GOJAK, Mirjana S. STAMENIĆ, and Vuk M. ADŽIĆ

Faculty of Mechanical Engineering, University of Belgrade, Belgrade, Serbia

The paper presents results of theoretical numerical research dealing with CO and NO_x emission performed in the process of optimization of the performance of low-power atmospheric burners.

The theoretical part of this paper, whose main goals were better understanding of the complex issues of methodology and establishment of performance prediction and optimization of low-power atmospheric gas burner included numerical variation of independent parameters, such as burner geometry, the coefficients of primary and secondary air and different gaseous fuels including biogas.

The findings of theoretically obtained performance prediction and optimization of atmospheric burners were experimentally investigated in purpose built test rigs for a number of variable parameters. The obtained results fully justified the proposed models of performance prediction and burner optimization.

Key words*: combustion, atmospheric burner, optimization, performance*

Introduction

In this paper the results of theoretical research performed within the process of optimizing the performance of low-power atmospheric burners are presented. In the theoretical phase, the main goals were to better understand the complex problems of atmospheric burner operation and to form a methodology for predicting the performance and optimization of low-power atmospheric burners, introducing burner geometry, primary, and secondary air coefficients, as well as gaseous fuel types including pure CH_4 (99.73 purity) [1] and biogas. Although this combustion system has a long tradition, is quite surprising that the issue of atmospheric burners is relatively modestly represented in the available literature. In this respect, the authors had no opportunity to compare their work with the some similar research of this issue in virtually all its aspects. The main objectives to be achieved by the construction and the development of modern atmospheric burners include the following categories: the stability of the work, the dynamic range of operation, emissions, lifetime of a burner, the degree of usefulness of the gas devices (consumers) in which the burner is to be installed, and the price of the burner. Design of a flexible burner incorporates a proper procedure and implementation of

_____
[*] Corresponding author, e-mail: amilivojevic@mas.bg.ac.rs

1892

Milivojević, A. M., *et al.*: Analysis of the Performance of a Low-Power …
THERMAL SCIENCE: Year 2021, Vol. 25, No. 3A, pp. 1891-1903

CFD codes but first of all understanding of chemical reactions that take place, how they affect the flame behaviour and how the flame interacts with the flow field.

The combination of commercially available chemical reactions, flow codes, and reduced chemical kinetics mechanisms with semi empirical models of low heat value fuels combustion were needed to be developed to enable reliable and fast numerical analysis of practical burners when more parameters are varied. Sub-task was defined as a fundamental research of chemical reaction mechanisms, modelling of emissions and flame structure in premixed combustion systems.

Modelling of premixed flame systems

Forming of the mathematical model or modelling of the combustion process, in this case consists of a fundamental part that includes: the phenomenology of chemical reactions and flame propagation, then variables that affect these phenomena (excess air coefficient, type of fuel, *etc.*). In premixed combustion, the fuel and oxidizer are already mixed at the molecular level before the fuel mixture is ignited. Combustion with a premixed flame is more complex for modelling than combustion with an unprmixed flame. Appropriate restrictions are set along with the goal [2]. The reason for this is that combustion with a premixed flame takes place in a thin layer whose geometry is affected by turbulence. In subsonic flows, the flame front propagation is determined by the laminar flame front propagation and turbulent vortices [3, 4]. The laminar flame front propagations determined by the complex effect of the simultaneous action of chemical reactions and the phenomenon of heat transfer and propagation with flow right next to reactants that have yet to enter the thermochemical reaction [5]. The effect of turbulence is reduced to the contraction and expansion of the flame in the laminar flame zone, increasing the laminar flame zone and, consequently, the effective flame front propagation [6, 7]. Large vortices tend to deform the laminar flame zone, while small vortices, if smaller than the thickness of the laminar flame, penetrate the laminar flame zone and intend to modify the laminar flame structure [8].

Modelling of chemical reactions, emissions of combustion products and flame structure

The goal of modelling

Flame structure and emissions were modelled using the CHEMKIN program (Reaction Design, Cal., USA). This program contains various models of chemical reactors. The one corresponding to the burner simulation with a laminar CH_4/air premixed flame was selected. This 1-D model of the reactor allows the calculation of: temperature profile, concentrations of the main components, intermediate elements and then flame propagation ratio as a function of distance. The flame structure and burner emissions with a laminar premixed CH_4/air flame [9] were calculated at an initial temperature of 298 K and at a pressure of 1.013×10^5 Pa [10]. The calculation was performed in the domain of 10 cm, which is significantly more than the thickness of the flame [11]. The coefficient of primary excess air λ' varied from 1.0 to 1.7. This data represents the input parameters of the executed calculation. The results of this numerical test are illustrated in figs. 1-10.

Based on the obtained results, it can be seen that the maximum values of the flame temperature decrease from 2080 K to 1700 K, fig. 11, with an increase in the coefficient of excess primary air λ' from 1.0 to 1.7. At the same time, the temperature profile gradients also decrease.
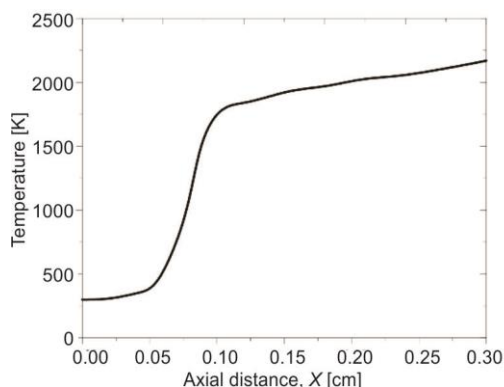
Figure 1. Temperature profile for $\lambda' = 1.0$

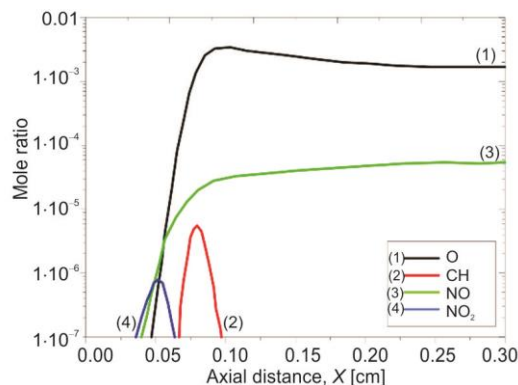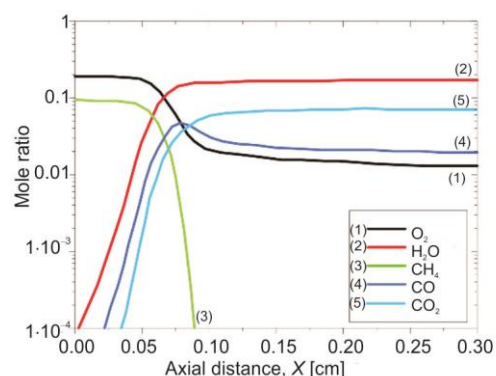**Figure 2. Concentration (O, CH, NO, NO_2) for $\lambda' = 1.0$**

Figure 3. Concentration (O_2, H_2O, CH_4, CO, CO_2) for $\lambda' = 1.0$
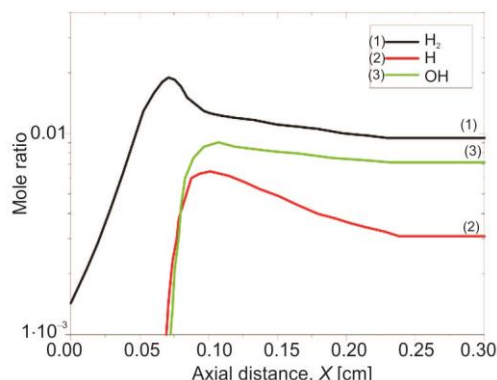

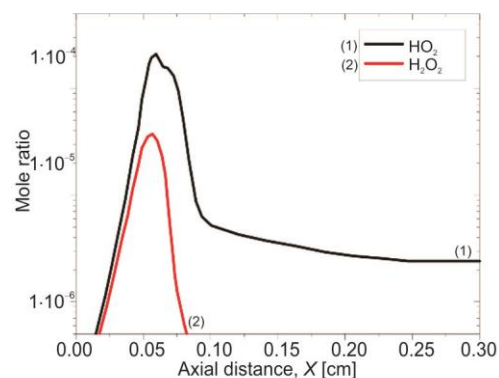**Figure 4. Concentration (H_2O, H, OH) for $\lambda' = 1.0$**

Figure 5. Concentration (HO_2, H_2O_2) for $\lambda' = 1.0$
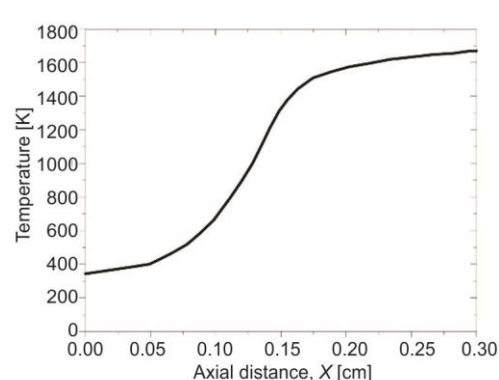

Figure 6. Temperature profile for $\lambda' = 1.7$

Combustion product concentration profiles also change with λ'. The maximum molar proportions of atomic oxygen (O) decrease from 0.34% to 0.09% with increasing λ'. The peaks are moved by approximately 0.1 to 0.2 cm above the burner with an increase in λ' of 1.0 to 1.7. Emissions of NO_x and CH radicals, as a function of distance, are shown in figs. 2 and 7. The NO_x almost entirely consist of NO which reaches a maximum for $\lambda' = 1$ and de-

1894

Milivojević, A. M., *et al.*: Analysis of the Performance of a Low-Power …
THERMAL SCIENCE: Year 2021, Vol. 25, No. 3A, pp. 1891-1903

creases to a minimum value for $\lambda' = 1.7$. The NO_2 concentration is negligible. A summary of the change in NO_x is given in fig. 12.
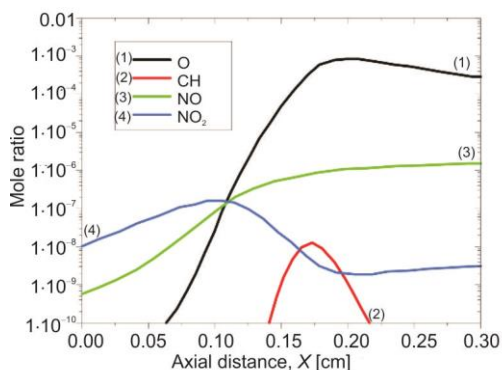

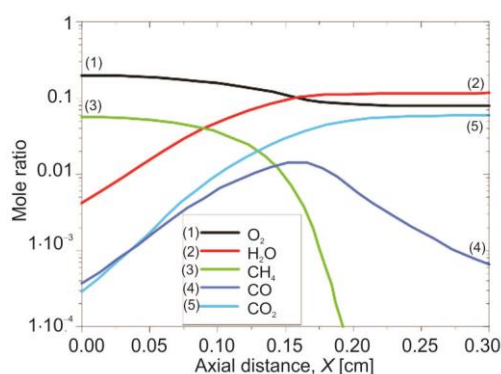**Figure 7. Concentration (O, CH, NO, NO_2) for $\lambda' = 1.7$**

Figure 8. Concentration (O_2, H_2O, CH_4, CO, CO_2) for $\lambda' = 1.7$
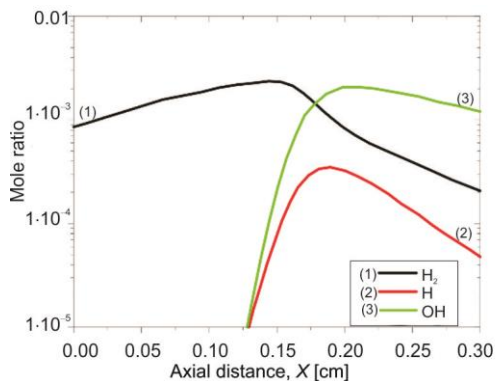

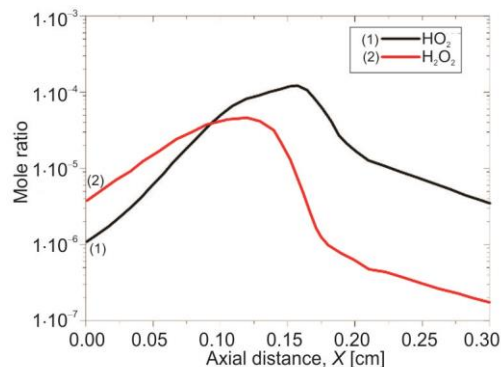**Figure 9. Concentration (H_2, H, OH) for $\lambda' = 1.7$**

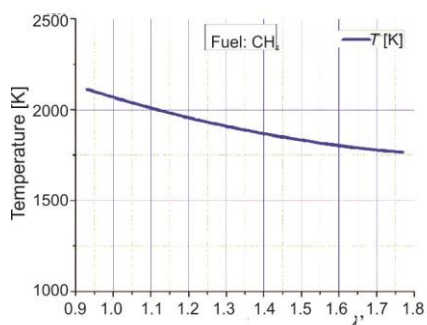**Figure 10. Concentration (HO_2, H_2O_2) for $\lambda' = 1.7$**

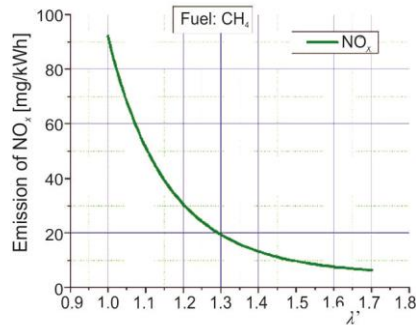**Figure 11. Change of flame temperature as a function of λ'**

Figure 12. Change of NO_x concentration as a function of λ'

The maximum values of CO concentration are in the flame zone. In the post-flame zone, CO is reduced to a level of about 2%, in the case of stoichiometric combustion, and to less than 1% for $\lambda' = 1.1$. With a further increase in λ', the value of CO concentration decreas-

Milivojević, A. M., *et al.*: Analysis of the Performance of a Low-Power …
THERMAL SCIENCE: Year 2021, Vol. 25, No. 3A, pp. 1891-1903

1895

es drastically. A summary of the change in CO is given in fig. 13. As a result of a smaller amount of fuel in the fuel mixture with increasing λ' the final concentrations of CO_2 and H_2O decrease. The CO_2 and H_2O concentrations decrease because the area with the higher temperature moves higher above the burner. The HO_2 and H_2O_2 are formed in the combustion zone and completely degrade after the combustion process is completed. The laminar flame front propagation rate as a function of the coefficient of primary excess air λ'is shown in fig. 14.
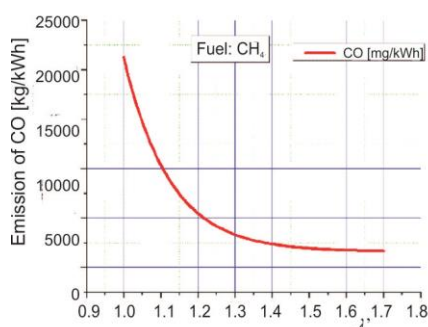

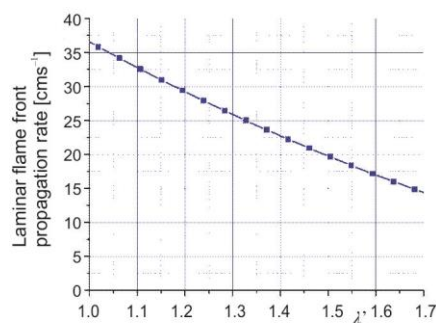**Figure 13. Change in CO concentration as a function of λ'**

Figure 14. Laminar flame front propagation rate as a function of λ'

Laminar flame front propagation rate, which is shown in fig. 14. as a function of the reciprocal value of the coefficient of excess air, *i.e.* size, which in Anglo-Saxon terminology is called equivalence ratio, shows slightly lower values for stoichiometric combustion conditions (λ' = 1) and slightly higher values for λ' = 1.7.

Fuel type effect

Flame structure and premixed flame emissions for Serbian natural gas

Calculations related to the structure of premixed flame and emission in burners with stable operation, during combustion of the mixture Serbian natural gas/air, were performed at an initial temperature of 298 K, at a pressure of 1.013×10^5 Pa, where, as in the previous case, the coefficient of excess primary air λ' is varied from 1.0 to 1.7. The composition of Serbian natural gas is given in the tab. 1.

Table 1. Composition of Serbian natural gas

Component	Vol.%
CH_4	84.37
C_2H_6	3.15
C_3H_8	0.44
C_4H_{10}	0.07
C_5H_{12}	0.02
N_2	1.95
CO_2	10.01

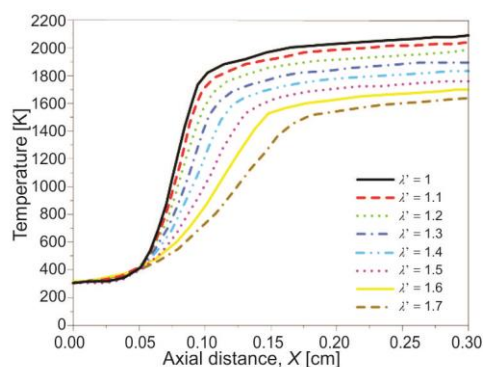The results of this numerical test are shown in figs. 15-18.

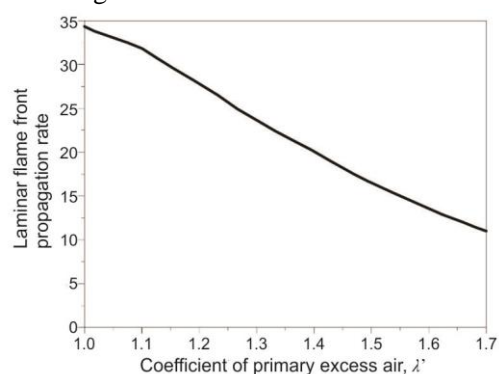**Figure 15. Flame temperature as a function of X and λ'**

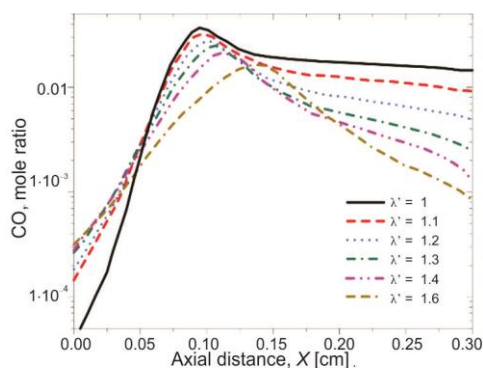**Figure 16. Change of laminar flame front propagation rate as a function of λ'**

Figure 17. CO emission depending on X and λ'
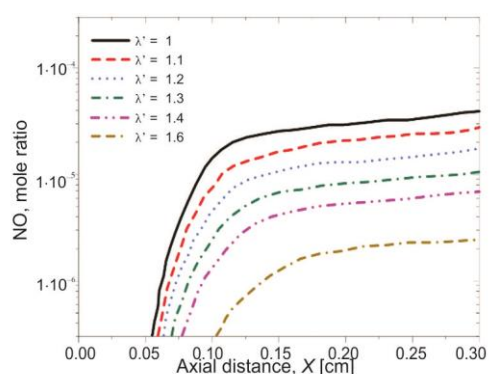

Figure 18. NO emission depending on X and λ'

Flame structure and emissions in premixed biogas flames

Biogas is a mixture of CH_4 and CO_2 in a ratio of 60% to 40%, respectively. The test results presented in this paper were obtained for a lean biogas/air mixture, and relate to flame front velocity, temperature profile, emission, and flame structure [12, 13]. The flame structure and combustion emissions [14], with a laminar premixed flame, of a lean biogas/air mixture [15] at an initial temperature of 298 K and a pressure of 1.013×10^5 Pa were calculated. The calculation was performed in the domain of 10 cm, which is significantly more than the thickness of the flame. The coefficient of excess primary air λ' varied from 1.0 to 1.5. The obtained results of this numerical test are shown in figs. 19-24.

From the presented results, figs. 19-24, for biogas, it can be seen that the laminar flame front propagation ratio is slightly lower in biogas than in pure CH_4, also NO_x emissions are lower while CO emissions are significantly higher in biogas than in CH_4. The flame temperature in biogas does not change much in relation to the flame temperature in CH_4.
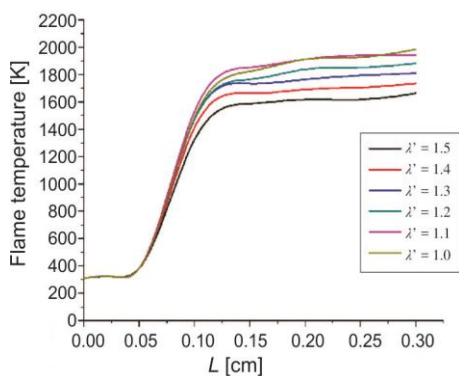
Milivojević, A. M., *et al.*: Analysis of the Performance of a Low-Power …
THERMAL SCIENCE: Year 2021, Vol. 25, No. 3A, pp. 1891-1903

1897

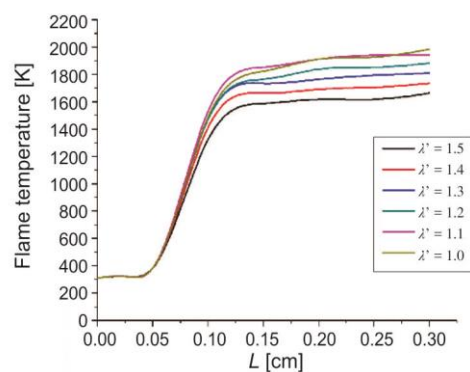**Figure 19. Flame temperature as a function of distance *L* and *λ*'**

Figure 20. Change of flame front propagation ratio as a function of distance *L* and *λ*'
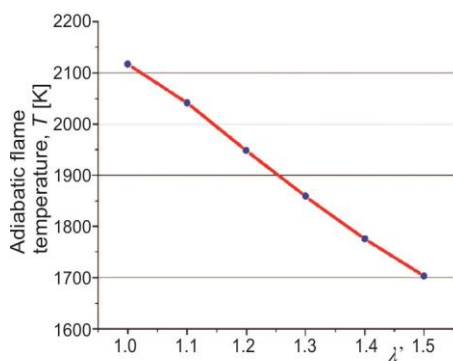
Figure 21. Change of adiabatic flame temperature as a function of *λ*'
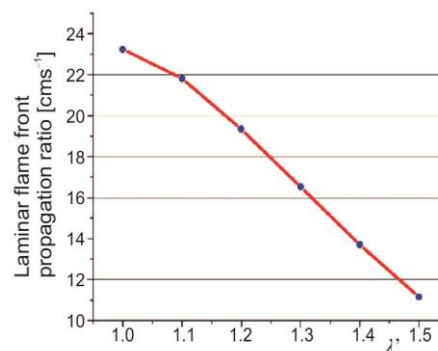

Figure 22. Change of the laminar flame front propagation ratioas a function of *λ*'
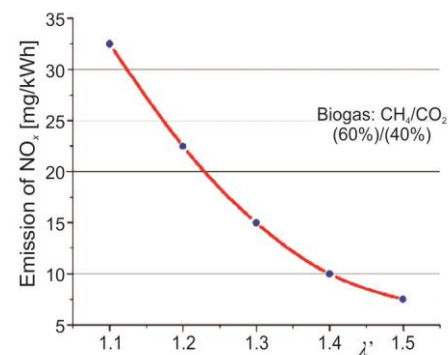

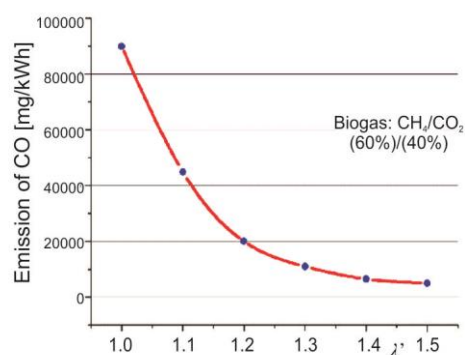**Figure 23. The NO$_x$ emission dependence of *λ*'**

Figure 24. The CO emission dependance of *λ*'

Methodology

Methodology of numerical optimization of the performance of an atmospheric burner basically consists of three tasks: forming an optimization model, application of the pro-

posed optimization model on a specific burner model, and validation of the proposed optimization model. Forming of the optimization model implies defining of the mathematical model which is then used for numerical analysis and the burner optimization. Research within the optimization of the atmospheric gas burner basically consists of two parts: determining the performance of burners in open space and determining the performance of the burner integrated in the chosen combustion chamber. In order to systematize and facilitate monitoring, this paper will present only the test details relevant to the optimization process. Based on the set requirements, in the project task, the preliminary construction of the burner was performed. The design of the burner depends on the required performance, the choice of burner construction and the type of fuel that the burner will use. Parameters such as burner design characteristics, burner thermal power, type of fuel, type of material from which the burner is made, *etc.*, have a direct impact on the performance and stability of the burner, whose numerical consideration leads to final conclusions and adoption of burner design. According to the adopted design solution of the burner, the numerical testing of the burner in different design conditions and operating modes is performed. The obtained results have an impact on the changes in the adopted design solutions, which are applied in the further evolutionary development of the burners, after which a re-experimental examination of the new adopted solutions will be tested.

Burner model

The development of the burner model assumes the definition of the geometry of all the elements of which the burner is made and their functional connection into the working unit with the appropriate required characteristics.

Modelling the formation of a mixture of fuel and air

This part of the paper will explain the basic principles of calculating the coefficient of excess primary air depending on the aerodynamic properties of the burner and the combustion chamber of the gas device in which the considered burner is installed [16]. The main task is to consider the influence of optimized quantities on the stability (combustion) of burners, efficiency, emission of pollutants (CO and NO_x) and the dynamic range of operation. The following were taken into account:
− Detailed burner geometry including fuel injector (nozzle, ejector, diffuser, burner body, flame ports surface).
− Working conditions (flow of fuel and air mixture, dynamic scope of work, type and composition of fuel, coefficient of excess primary air) [17].
− Interaction between geometry and aerodynamics.

Burner model

For practical application when dimensioning the burner elements, we move on to a simplified one-dimensional consideration of the internal aerodynamics of the gas burner-combustion system. The construction scheme of the ALFA 9 burner gas heater system is given in fig. 25.
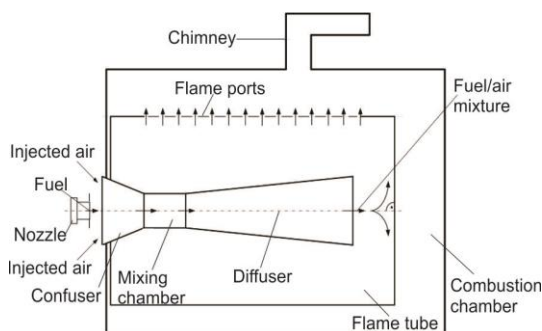

Figure 25. Optimized burner in the combustion chamber of the gas heater ALFA 9

Influential parameters

The parameters that affect the achievement of the previous goals are: work pressure, type of fuel, nozzle selection, distance of the nozzle from the mixer, type of mixer, and bsurface of flame ports surface. These parameters in a complex way affect the performance of the burner.

Considering that atmospheric burners are mainly intended for households and that their thermal power ranges from 8 to 12 kW. Atmospheric burner manufactured by BCT from Netherlands was selected. The initial elements of the burner geometry are defined by the initial quantities. The details are: thermal power of the burner 10.2 kW.

In order to achieve the property of multi-fuel, various gaseous fuels were used during the test: commercial mixture of propane and butane (LPG), Serbian natural gas, biogas. The dynamic range of the burner should be 1:3. The NO_x and CO emission limit values are 50 mg/kWh, respectively.

The propagation of the flame front is modelled by solving the transport equation in which the process variable appears. Namely, the variable that appears in the equation, denoted by, is called the process variable and represents the total amount of combustion products expressed in mass percentages, averaged with the equilibrium mass fractions of combustion products. This equation has the following form:

$$\frac{\partial}{\partial t}\left(\rho c\right)+\nabla\left(\rho \vec{v} c\right)=\nabla\left(\frac{\mu_t}{\mathrm{Sc}_t}\nabla c\right)+\rho \mathrm{Sc} \tag{1}$$

Process variable is defined as the normalized sum of combustion products:

$$c = \frac{\sum\limits_{i=1}^{n} Y_i}{\sum\limits_{i=1}^{n} Y_{i,\mathrm{eq}}} \tag{2}$$

By definition, $c = 0$ in the non-combustion zone, in the zone where the combustion of the fuel mixture is completed: $c = 0$ – unburned fuel mixture, $c = 1$ – burnt fuel mixture.

The value of the process variable c is given as a boundary condition for all input quantities in the considered system. Usually the value of c is specified either as 0 (unburned fuel mixture) or as 1 (burned fuel mixture).

The mean value of the reaction in eq. (1), is given as:

$$\rho \mathrm{Sc} = \rho_u U_t \left|\nabla c\right| \tag{3}$$

Based on the semi-empirical approach and eq. (1), the characteristics of the optimized burner were calculated in order to predict its performance and their harmonization with the required set values at the beginning of the work. This calculation included the coefficient of primary excess air as a function of: thermal power of the burner, nozzle diameter, the diameter of the Venturi tube neck, burner flame ports surfaces and pressure drop in the burner. The CH_4, biogas with composition of 60% CH_4 and 40% CO_2 [19] and propane C_3H_8 were used as base fuel in the calculation.

Coefficient of primary excess air λ'

The resistance to the flow through the burner affects the value of the coefficient of primary excess air λ'. Based on the calculation presented in previous chapter, figs. 26-28 are obtained, which show the relationship between the coefficient of friction determined on the

basis of the normal flow rate through the flame ports and the coefficient of primary excess air λ' for different types of gaseous fuel (CH_4, biogas: 40% CO_2 + 60% and C_3H_8). On fig. 29 dependence of the coefficient of primary excess air on the changes of the flame ports surface at a constant burner heat output of 10.2 kW, for the different fuel types [20].
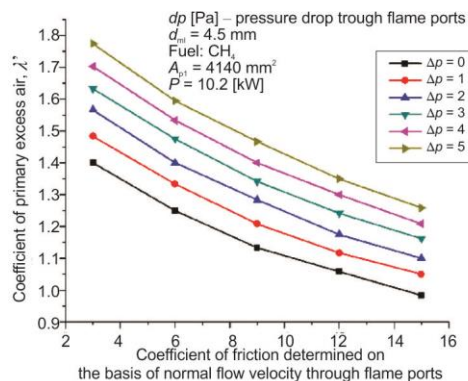

Figure 26. Coefficient of primary excess air as a function of pressure drop and coefficient of friction
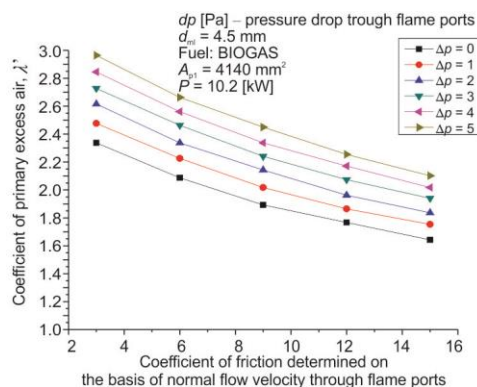

Figure 27. Coefficient of primary excess air as a function of pressure drop and friction coefficient for biogas IZ PDF
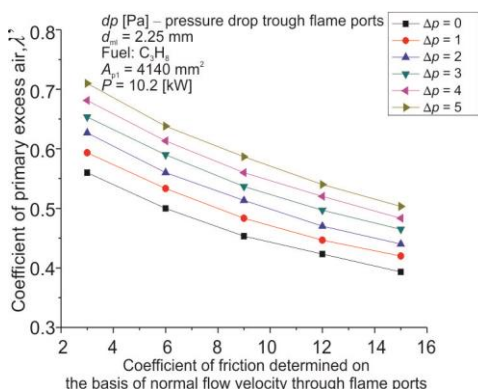

Figure 28. Coefficient of excess primary air as a function of pressure drop and coefficient of friction for C_3H_8
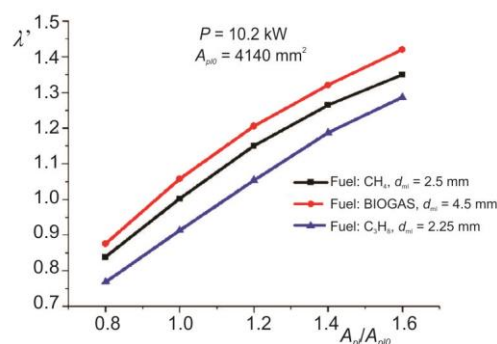

Figure 29. Coefficient of primary excess air as a function of increasing the initial surface area of the flame ports A_{pl} / A_{pl0}.

Analysis of the presented results

Based on the obtained results, the following analysis was performed. Figures 30 and 31 show the dependence of the average mixture flow rate through the flame ports $u_{AV.DIS}$. The flame front propagation rate u_{FP}, as well as the change in the excess air coefficient λ depending on the change in the flame ports surface of the burner A_{pl}/A_{pl0}. Two cases were considered: operating mode at maximum power $P = 10.2$ kW and operating mode at three times lower power $P = 3.4$ kW, which corresponds to a dynamic burner operating range of 1:3.

It can be seen, in fig. 30, that at a power of 3.4 kW (fuel: 100% CH_4) the average flow rates of fuel/air mixture through the flame ports $u_{AV.DIS}$ and flame front propagation rate u_{FP} intersect at the value $A_{pl}/A_{pl0} = 1.033$. Until $A_{pl}/A_{pl0} = 1.033$ we can see that $u_{FP} > u_{AV.DIS}$ and flame retraction phenomena occurs (Flash back), from $A_{pl}/A_{pl0} = 1.033$ is $u_{FP} < u_{AV.DIS}$ and

we have a lifting of the flame, and with further increase A_{pl}/A_{pl0} ($A_{pl}/A_{pl0} > 1.6$) we would have an increasing difference between u_{FP} and $u_{AV.DIS}$, so at one point ($u_{FP} << u_{AV.DIS}$) the flame would be a blown away (blow off).

On fig. 31, it can be seen that at a power of 10.2 kW (fuel: 100% CH_4) the average flow rates of fuel/air mixture through the flame openings in the $u_{AV.DIS}$.and the flame front propagation rate u_{FP} do not intersect, but all the time $u_{FP} < u_{AV.DIS}$, which means that we have a lifted flame all the time, and with the further increase in A_{pl}/A_{pl0} ($A_{pl}/A_{pl0} > 1.6$) we would have an increasing difference between u_{FP} and $u_{AV.DIS}$, so at one point ($u_{FP} << u_{AV.DIS}$) the flame would be a blown away (blow off).
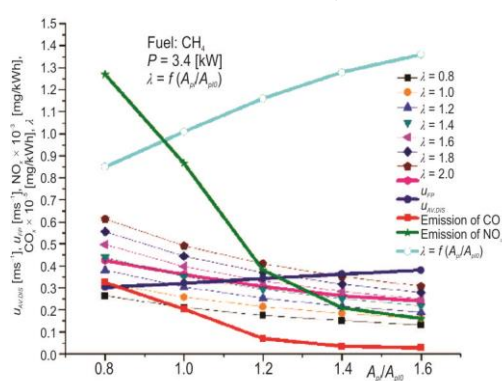

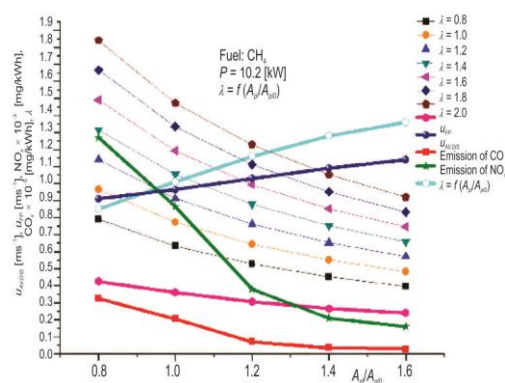**Figure 30. Dependence of $u_{AV.DIS.}$, u_{FP}, λ, CO, and NO$_x$ emissions on A_{pl}/A_{pl0} for CH$_4$ at power of P = 3.4 kW**

Figure 31. Dependence of $u_{AV.DIS.}$, u_{FP}, λ, CO, and NO$_x$ emissions on A_{pl}/A_{pl0} for CH$_4$ at power of P = 10.2 kW

The same consideration was applied when using biogas with a composition of 60% CH_4 and 40% CO_2. The dependence of the average flow rate of fuel/air mixture through the flame openings $u_{AV.DIS.}$, the flame front propagation rate u_{FP}, as well as the change in the coefficient of excess air λ depending on the change in the flame ports surface of the burner A_{pl}/A_{pl0} are shown in figs. 32 and 33.
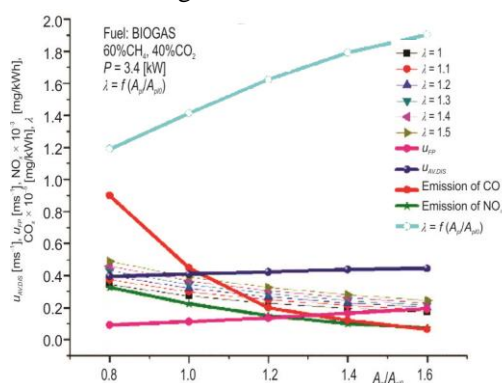
Figure 32. Dependence of $u_{AV.DIS.}$, u_{FP}, λ, CO, and NO$_x$ emissions on A_{pl}/A_{pl0} for biogas at power from P = 3.4 kW
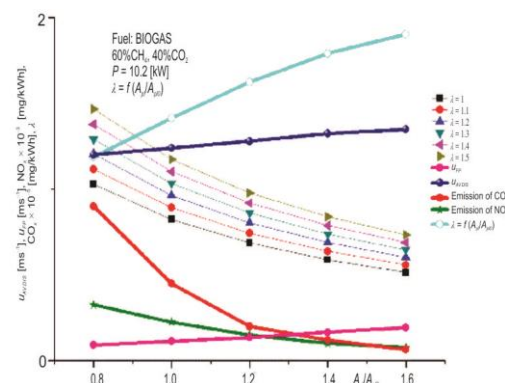

Figure 33. Dependence of $u_{AV.DIS.}$, u_{FP}, λ, CO, and NO$_x$ emissions on A_{pl}/A_{pl0} for biogas at power from P = 10.2 kW

It can be seen, on fig. 32, that at a power of 3.4 kW (fuel: biogas composition of 60% CH_4 and 40% CO_2) the average flow rates of fuel/air mixture through the flame ports

1902

Milivojević, A. M., *et al.*: Analysis of the Performance of a Low-Power …
THERMAL SCIENCE: Year 2021, Vol. 25, No. 3A, pp. 1891-1903

$u_{AV.DIS}$ and the flame front propagation rates u_{FP} do not intersect, but all the time $u_{FP} < u_{AV.DIS}$, which means that we have a turbulent flame lifted all the time. It is also visible that at this power both curves with increasing A_{pl}/A_{pl0} keep almost the same trend so there will be no flame blow off phenomenon.

Also on fig. 33, it can be seen that at a power of 10.2 kW (biogas fuel composition 60% CH_4 and 40% CO_2), the average flow rates of fuel/air mixture through the flame ports $u_{AV.DIS}$ the flame front propagation rates u_{FP} do not intersect but all the time there is $u_{FP} < u_{AV.DIS}$, although there is a larger difference in the values of $u_{AV.DIS}$ and u_{FP} in relation to the power of 3.4 kW, which means that we have a turbulent flame lifted all the time, it is also visible that at this power both curves with the increase of A_{pl}/A_{pl0} keep almost the same trend so that the blow off of flame will not occur.

Conclusions

The influence of the mentioned elements on the stability of burner operation and NO_x and CO emissions was analysed. Based on these analyses, an optimization method has been developed whose functions are to increase the stability of the optimized atmospheric burner and meet the limit values of NO_x and CO emissions. Based on performed theoretical analyses, a method for optimizing the performance of low-power multifuel atmospheric burners has been formed and numerical research had been performed. The obtained results of this numerical research were used for construction of the prototype burner. Based on these calculations, reconstructive improvements are made to the burner prototype and the first stage of burner evolution is obtained. In addition experimental verification of the proposed burner prototype were performed in order to confirme needed performances of this burner. This optimization method fully confirmed the quality of the proposed performance optimization methodology in terms of stability, dynamic range and emissions, which is also contributing to increase of the energy efficiency of low-power gas appliances and meet environmental requirements, *i.e* sustainable development.

Procedure can be repeated as many times as necessary to obtain the final prototype of the burner that has the required performance, defined in the optimization task and confirmed on the test bench and in the gas appliance for which the burner is optimized. Theoretical optimization of the burner was performed by this procedure. The extent to which the theoretical approach provided a methodology for optimizing atmospheric burners can be confirmed by appropriate experimental research.

Nomenclature

A_{pl0} – initial area of the flame ports surface, [mm^2]

A_{pl} – area of the flame ports surface, [mm^2]

c – process variable size of the observed chemical reaction, [–]

d_{ml} – nozzle diameter, [mm]

L – distance, [cm]

n – number of combustion products, [–]

P – power of the burner, [kW]

Δp – pressure drop on the nozzle, [Pa]

Sc_t – turbulent Schmidt number, [–]

Sc – member of the equation that describes the formation of a process variable, [s^{-1}]

U_t – turbulent flame velocity, [ms^{-1}]

$u_{AV.DIS}$ – average flow rates of fuel/air mixture through the flame ports, [ms^{-1}]

u_{FP} – flame front propagation rate, [ms^{-1}]

Y_i – mass fraction of ith combustion product, [–]

$Y_{i,eq}$ – equilibrium mass fraction of the ith combustion product, [–]

Greek symbols

λ' – coefficient of primary excess air, [–]

ρ_u – density of unburned fuel mixture, [kgm^{-3}]

References

[1] Andrews, G. E., *et al.*, The Burning Velocity of Methane-Air Mixtures, *Combustion and Flame*, *19* (1972), 2, pp. 275-288
[2] Tanino, T., Sensitivity Analysis in Multiobjective Optimization, *Journal of Optimization Theory and Applications*, *56* (1988), Mar., pp. 479-499
[3] Sanchez A. L., *et al.*, The Reduced KineticmDescription of Lean Premixed Combustion, *Combustion and Flame*, *123* (2000), 4, pp. 436-464
[4] Lytras, I., P. *et al.*, Reduced Kinetic Models for Methane Flame Simulations, *Combustion, Explosion, and Shock Waves*, *55* (2019), 2, pp. 132-147
[5] Franzelli, B. G., Impact of the Chemical Description on Direct Numerical Simulations and Large Eddy Simulations of Turbulent Combustion in Industrial Aero-Engines, Ph. D. thesis, French National Centre for Scientific Research, Paris, France, 2011
[6] Allauddin, U., Modelling of Turbulent Premixed Combustion Using LES and RANS Methods, Ph. D. thesis, Universitätsbibliothek der Universität der Bundeswehr, Munchen, Germany, 2017
[7] Miake-Lye, R. C. *et al.*, Lifted Turbulent Jet Flames: A Stability Criterion Based on the Jet Large-Scale Structure, *Proceedings*, 22nd Symposium (International) on Combustion, Combustion Institute, Pittsburgh, Penn., USA, 1988, pp .817-824
[8] Zimont, V. L., Gas Premixed Combustion at High Turbulence. Turbulent Flame Closure Combustion Model, *Experimental Thermal and Fluid Science, 21* (2000), 1-3, pp. 179-186
[9] Fackler, K. B., *et al.*, NO_x Behavior for Lean-Premixed Combustion of Alternative Gaseous Fuels, *Journal of Engineering for Gas Turbines and Power, 138* (2015), 4, pp. 1-30
[10] Zimont, V., *et al.*, An Efficient Computational Model for Premixed Turbulent Combustion at High Reynolds Numbers Based on a Turbulent Flame Speed Closure, *Gas Turbines Power, 120* (1998), 3, pp. 526-532
[11] Wu, W. W., *et al.*, Experimental Investigation of Premixed Methane-Air Combustion Assisted by Alternating-Current Rotating Gliding Arc, *IEEE Transactions on Plasma Science, 43* (2015), 12, pp. 3979-3985
[12] Zimont, V. L. *et al.*, A Numerical Model of Premixed Turbulent Combustion of Gases, *Chem. Phys. Reports*, *14* (1995), 7, pp. 993-1025
[13] Umyshev, D. R., *et al.*, Effects of Different Fuel Supply Types on Combustion Characteristics Behind Group of V-Gutter Flame Holders: Experimental and Numerical Study, *Thermal Science*, *24* (2020), 1A, pp. 379-391
[14] Kuznetsov, V. R., *et al.*, *Turbulence and Combustion*, Hemisphere Publ., Corp., New York, USA, 1990
[15] Marsh, R., *et al.*, Premixed Methane Oxy-Combustion in Nitrogen and Carbon Dioxide Atmospheres, Measurement of Operating Limits, Flame Location and Emissions, *Proceedings of the Combustion Institute*, 36 (2017), 3, pp. 3949-3958
[16] Suckart, D., *et al.*, Modelling Turbulent Premixed Flame-Wall Interactions Including Flame Quenching and Near-Wall Turbulence Based on a Level-Set Flamelet Approach, *Combustion and Flame, 190*, (2018), Apr., pp. 50-64
[17] Zimont, V. L., *et al.*, Modelling Turbulent Premixed Combustion in the Intermediate Steady Propagation Regime, *Progress in Computational Fluid Dynamics, An International Journal*, *1* (2001), 1, pp. 14-28
[18] Jovanović, R. D., *et al.*, Experimental and Numerical Investigation of Flame Characteristics During Swirl Burner Operation Under Conventional and Oxy-Fuel Conditions, *Thermal Science*, *21* (2017), 3, pp. 1463-1477
[19] Jiang, X., *et al.*, The Combustion Mitigation of Methane as a Non-CO_2 Greenhouse Gas, *Progress in Energy and Combustion Science*, *66* (2018), May, pp. 176-199